Phosphorus limitation determines the quality of dissolved organic matter released by marine heterotrophic prokaryotes

Nawal Bouchachi, Ingrid Obernosterer, Barbara Marie, Olivier Crispi, Eva Ortega-Retuerta

Phosphorus limitation determines the quality of dissolved organic matter released by marine heterotrophic prokaryotes.

Running head: Phosphorus effects on prokaryotic DOM

Nawal Bouchachi[1*], Ingrid Obernosterer[1], Barbara Marie[1], Olivier Crispi[1], Eva Ortega-Retuerta[1*]

[1]CNRS/Sorbonne Université, UMR7621 Laboratoire d'Océanographie Microbienne, Banyuls sur Mer, France.

*Correspondence: nawal.bouchachi@obs-banyuls.fr , ortegaretuerta@obs-banyuls.fr

Author Contribution Statement: NB, IO and EOR conceived the work. NB and EOR performed the experiments with an active contribution of BM and OC to chemical analyses. NB analyzed data and wrote the paper with significant contributions from IO and EOR.

Scientific Significance Statement

Marine heterotrophic prokaryotes (HP) generate copious amounts of dissolved organic matter (DOM). Some of this DOM is recalcitrant to biological degradation and can persist in the ocean for millennia. This carbon sequestration mechanism is called the microbial carbon pump (MCP). The factors controlling the strength of the MCP are still poorly understood. Phosphorus (P) limitation is a common condition in the ocean that can influence HP growth and metabolism. We addressed here the question of whether P-limitation affects the quantity and quality of DOM released by HP. We found no effect of P-limitation on HP-derived DOM net quantity. However, using fluorescence spectroscopy, we demonstrated that P-limitation altered DOM composition with an increase in humic-like compounds. Our study provides experimental evidence that P availability plays an important role in shaping the chemical composition of HP-derived DOM. Our results have implications for the fate of HP-derived DOM in the ocean, suggesting that P-limitation is a key driver of the MCP.

Data availability statement

Data and metadata are available in the Dryad repository at https://doi.org/10.5061/dryad.xsj3tx9h4

The PARAFAC model is available in the OpenFluor Database at http://openfluor.org

Abstract

We determined phosphorus (P) limitation effect on the quantity and quality of dissolved organic matter (DOM) released by heterotrophic prokaryotes (HP). We grew 2 single bacterial strains from different lifestyles, the copiotrophic *Photobacterium angustum* and the oligotrophic *Sphingopyxis alaskensis*, and natural HP communities collected in fall and spring from the Mediterranean Sea, on glucose under 2 treatments: P-replete vs. P-limiting. DOM release by HP comprised up to 30 % of the initial carbon provided for growth. P availability influenced carbon allocation to different cellular processes (respiration vs. growth), but did not significantly affect the net quantity of DOM released by HP. However, using fluorescence spectroscopy, we demonstrated an effect of P-limitation on DOM quality, with a predominance of humic-like compounds under P-limitation but protein-like compounds under P-repletion. Our results suggest that P-limitation could determine the fate of HP-derived DOM in the ocean, thus affecting the microbial carbon pump.

Keywords

Dissolved organic matter, phosphorus limitation, heterotrophic prokaryotes, fluorescent dissolved organic matter.

Introduction

Dissolved organic matter (DOM) is the dominant pool of reduced carbon in the ocean. DOM covers a continuum of reactivity ranging from labile, with fast turnover, to recalcitrant DOM that persists for millennia being thus a carbon sequestration mechanism (Hansell, 2013). Heterotrophic prokaryotes (HP) are important drivers of DOM biogeochemical cycling in the ocean (Nagata, 2008). They process about half of the carbon fixed by primary producers (Cole, et al., 1988), converting it into CO_2 (respiration) and new biomass (production). The fraction of carbon converted into new biomass, defined as the prokaryotic growth efficiency (PGE), is crucial for estimating carbon fluxes in the ocean (del Giorgio & Cole, 1998). But HP also release a myriad of DOM compounds, part of which can be recalcitrant and thus be stored in the ocean (Ogawa, 2001; Gruber et al., 2006; Lønborg et al., 2009; Lechtenfeld et al., 2015; Osterholz et al., 2015). This process, termed the microbial carbon pump (Jiao et al., 2010), may be an important carbon sequestration mechanism.

In recent years, different fractions of this HP-derived DOM (HP-DOM) have been characterized, e.g. amino acids concentration (Daoud & Tremblay, 2019), molecular signature (Lechtenfeld et al. 2015; Koch et al. 2014) and fluorescence properties (Shimotori et al., 2009). This last technique has allowed characterizing HP-DOM quality (Rochelle-Newall and Fisher 2002; Kramer and Herndl 2004; Shimotori et al., 2009) and has revealed differences in fluorescent DOM (FDOM) related to the taxonomy of the producing HP (Shimotori et al., 2012; Goto et al., 2020; Ortega-Retuerta et al., 2021). Yet, the reason why FDOM is released and its relation to environmental factors has been scantly studied.

HP can release DOM as a direct by-product of their biosynthesis and growth (Kawasaki and Benner 2006) or by the imbalance between their anabolism and catabolism (Carlson et al.,2007). Viral lysis and sloppy grazing by protozoans can also release DOM from HP (Middelboe & Jørgensen, 2006; Nagata, 2000) and alter its composition (Gruber et al., 2006; Heinrichs et al., 2022).

However, many molecules can also be released for specific needs including competition (antibiotics), communication, nutrient acquisition (siderophores, ectoenzymes) (Kujawinski 2011; Carlson 2002). Therefore, the quantity and chemical nature of HP-DOM could differ as a function of environmental conditions such as nutrient availability. Phosphatase synthesis, for instance, is highly influenced by phosphorus (P) limitation (Romano et al., 2015). Although P-limitation for HP is a dominant condition

in the ocean (Wu et al., 2000; Obernosterer et al., 2003; Lazzari et al., 2016), its effect on HP-DOM quantity and chemical composition is unclear (e.g. Thompson & Cotner, 2020). For example, Romano et al. (2014), looking at solid-phase extracted DOM, showed changes in bacterial metabolomes induced by P-limitation, with an increase in phenolic and polyphenolic compounds. Therefore, we hypothesize that P availability would have an effect on DOM quantity and quality.

To test this hypothesis, we addressed two main questions: (i) Does P-limitation affect the quantity of DOM released by HP? (ii) Do the fluorescence properties of HP-DOM depend on P availability?

Material and methods

Experimental design

To test the effect of P-limitation on HP-DOM, we performed 4 experiments using 2 model bacterial strains and 2 natural HP communities.

The two bacterial strains were obtained from the "Laboratoire Arago culture collection": *Photobacterium angustum S14*, a copiotrophic *Gammaproteobacterium* isolated from coastal waters (Botany Bay, Australia) (Lauro et al., 2009) ; and *Sphingopyxis alaskensis RB2256*, an oligotrophic *Alphaproteobacterium* isolated from North Pacific waters (Eguchi et al., 2001). They were chosen based on their capacity to grow on glucose, the availability of their genome sequenced, and the ample experience culturing them at our laboratory (e.g. Koedooder et al., 2018; Matallana-Surget et al., 2012). Initially preserved in glycerol (33% final concentration) at -80 °C, they were thawed and 2 consecutive acclimation steps (strains inoculated in fresh media, dilution 1:1000) were performed prior to experiments to minimize glycerol presence in the final incubations.

The natural HP communities were collected from surface waters of a coastal site located in the NW Mediterranean Sea (SOLA, 42°29'300 N – 03°08'700 E) at 2 different seasons, fall (November 2020) and spring (May 2021), referred to as SOLA-fall and SOLA-spring experiments respectively. Water was prefiltered, immediately after sampling, by 0.8 µm and then cells were concentrated from ~3000 mL to ~40 mL by filtering through 0.2 µm filters to allow low inoculum volume, minimizing thus

nutrient and DOM supply from seawater to the media. The natural communities were then directly inoculated in the experimental media (dilution 1:1000).

Both strains and communities were grown separately on minimum media (Fegatella et al., 1998) consisting of artificial sea water (composition in Table S1) with glucose as a sole carbon (C) source (~ 200 µmolC L^{-1}), nitrogen as NH_4Cl (~ 40 µmol L^{-1}), P as $NaHPO_4$, trace metals and vitamins. Two experimental treatments were considered, termed "balanced" and "unbalanced", by changing the initial P concentration in the media. In the "balanced" treatment, P was added at an initial concentration of ~ 4.4 µmol L^{-1}, thus inorganic nutrients were at a C:N:P ratio of 45:9:1, mimicking the internal stoichiometry of HP cells (Goldman et al. 1987). In the "unbalanced" treatment, P was added at an initial concentration of ~ 0.53 µmol L^{-1}, so C:N:P ratios were at ~ 374:75:1, similar to the mean C:P ratio of bulk DOM in the surface ocean (Hopkinson & Vallino, 2005).

Culture media were inoculated at an initial cell abundance of 0.5 to 9 $x10^4$ cells mL^{-1} for the strains and of 0.4 to 2 $x10^4$ cells mL^{-1} for the natural communities. Two contamination controls per treatment (i.e. culture media with no cell inoculum) were also incubated in parallel. Incubations were set up in combusted (5 hours at 450 °C) 500 mL glass bottles, in triplicate (except for *S. alaskensis*, 4 replicates) at 25 °C in the dark and shaken at 100 rpm.

Cell growth was determined by flow cytometry (See Supporting Information) and experiments were conducted until the stationary phase was reached.

To quantify and characterize the HP-DOM, samples were taken at the beginning of the experiment (T_0), and in the stationary phase (T_f). At T_0, samples for HP-DOM were directly taken from the cultures while at T_f, samples were collected after filtering the cultures twice onto pre-rinsed 0.2 µm polycarbonate filters using pre-combusted all-glass vacuum filtration unit (Millipore). Negligible DOM leaching from the polycarbonate filters was previously tested (data not shown). The double filtration procedure ensured minimal cell presence in the filtrates (< 2 % of the abundance before filtration).

Chemical analyses

Samples for dissolved organic carbon (DOC) were acidified and stored in the dark at room temperature until analysis by temperature catalytic oxidation technique (Benner & Strom, 1993). Glucose was quantified as μmol L^{-1} of carbon equivalent (C-glucose) based on an adapted colorimetric method (Myklestad et al. 1997). Inorganic nutrients (NH_4^+, NO_3^-, NO_2^-, PO_4^{3-}) were also measured. Detailed chemical analyses are provided in Supporting Information.

FDOM measurement

FDOM samples were analyzed within few hours upon sampling. Excitation emission matrices (EEMs) were recorded using a JASCO FP-85000 Spectrofluorimeter in a 10 mm quartz cell at scan speed of 5000 nm min^{-1}. Excitation scans ranged between 240 to 450 nm at 5 nm intervals and emission scans were recorded between 300 to 560 nm at 2 nm intervals. MilliQ EEM blanks were recorded in every batch of analysis. Fluorescence intensities were reported in Raman units (RU) obtained by dividing the fluorescence units by the MilliQ blank peak area (Raman scatter) excited at 350 nm. EEMs were measured for all replicates except in SOLA-fall experiment where only one EEM per treatment was recorded (See supporting information).

Data analyses

Growth rates were calculated as the slope of the ln-transformed cell abundances over time. The prokaryotic growth efficiency was determined as the increase of biomass from the lag phase to the maximum growth reached, divided by the decrease of C-glucose between T_0 and T_f following this equation:

$$\mathrm{PGE}\ (\%) = \frac{\Delta\ \text{biomass}\ (\mu\text{mol}\ L^{-1})}{\Delta\ \text{C-glucose}\ (\mu\text{mol}\ L^{-1})} \times 100$$

where biomass was obtained using specific cell to biomass conversion factors for each experiment (Table S2).

HP-DOM release was quantified as the difference between the concentration of C-glucose remaining at the end of the experiment and bulk DOC concentration (DOC excess) as follows. Our calculation assumes that HP did not release carbon as glucose and other monosaccharides during the incubation.

$$\text{HP-DOM } (\mu\text{mol L}^{-1}) = \text{DOC}_{tf} \ (\mu\text{mol L}^{-1}) - \text{C-glucose}_{tf} \ (\mu\text{mol L}^{-1})$$

To better understand FDOM characteristics, EEMs were separated into distinct components using parallel factor analysis (PARAFAC) under the drEEM toolbox in MATLAB (Murphy et al., 2013). A 6-component model (Table S3, Fig S2) was validated and associated to identified components in previous studies published in the OpenFluor database (Detailed method in Supporting information). Differences in biological and chemical parameters between the experimental treatments were tested by one-way analysis of variance (ANOVA) and post-hoc Tukey tests.

We performed linear regression analysis between the FDOM components and the HP growth rates, pooling data from all experiments. A correspondence analysis (CA) was applied to the identified components and their maximum intensity for each experiment. Statistics were performed using R 3.6.1 (R Core Team, 2019) and the FactoMineR (v.2.3; Lê et al., 2008) package.

Results

Heterotrophic prokaryotic growth

Independent of nutrient regime, *P. angustum* and SOLA-fall grew fast, reaching the stationary phase after 30 h of incubation (Fig. 1a, c), while SOLA-spring only plateaued after 60 h of incubations (Fig. 1d). *S. alaskensis* grew slower and reached the stationary phase after about 100 h (Fig. 1b). In the contamination controls, cell numbers remained < 16 $x10^4$ cells mL^{-1}. The maximum cell abundance reached was always higher in the balanced than in the unbalanced treatments (*P. angustum*, p-value <0.05; *S. alaskensis*, SOLA-fall and SOLA-spring, p-value <0.001). P-limitation did not affect the growth rates in any of the incubations (Table 1), but *S. alaskensis* grew significantly slower than *P. angustum* and the natural HP communities (p-value <0.001). In the unbalanced (P-limited) treatments,

193 PGE was always significantly lower than in the balanced treatments (Table 1, *P. angustum*, p-value
194 <0.05; *S. alaskensis* p-value <0.001; SOLA-fall p-value <0.001; SOLA-spring, p-value <0.01).
195
196 *HP-DOM quantity*
197
198 At the end of the incubations, 1.8 to 23.4 µmol L^{-1} of initial C-glucose remained, while DOC
199 concentrations ranged between 18.2-64.6 µmol L^{-1} (Table S4). The single strains released between 50.5
200 to 60.2 µmol C L^{-1}, corresponding to 20 - 30 % of initial C-glucose (Table 1). For the natural HP
201 communities, DOC release ranged between 5.3 and 43.2 µmol L^{-1} (3 - 18 % of initial C-glucose), which
202 is significantly lower than the release by the strains (p-values <0.05). P-limitation did not significantly
203 affect the net quantity of HP-DOM (Table 1).
204
205 *HP-DOM fluorescence quality*
206
207 FDOM signals were negligible at the onset of the experiments, but these were markedly noticeable at
208 T_f (Fig S1). Thus, we considered this fluorescence as derived from HP. The fluorescent signal at T_f was
209 decomposed into 6 fluorescence components with distinct properties (Fig S2; Table S3): C_{340} (ex
210 275/em 340, protein-like DOM); C_{460} (ex 270 (385)/em 460, fulvic-like DOM); C_{354} (ex 290/em 354,
211 protein- or phenolic-like DOM); C_{398} (ex 315/em 398, microbial humic-like DOM); C_{440} (ex 340
212 (265)/em 440, humic-like DOM); and C_{424} (ex 250/em 424, humic-like DOM).
213 The DOM released by *P. angustum* and HP communities SOLA-fall and SOLA-spring was enriched in
214 protein-like C_{340} and humic-like C_{424} components, in contrast to *S. alaskensis* that rather released DOM
215 enriched in humic-like C_{460} and C_{398} components, as shown by the CA (Fig. 2).
216 EEMs in the unbalanced treatment showed a more humic-like signature (except SOLA-spring, Fig 3a).
217 DOM released under balanced conditions was significantly enriched in the protein-like component C_{340},
218 compared to unbalanced, in all experiments except for *S. alaskensis* (Fig. 3b). Conversely, we detected
219 higher microbial humic-like C_{398} in the unbalanced treatment in both single strains and SOLA-fall, but
220 not in SOLA-spring (Fig. 3d). Humic-like components C_{460} and C_{440} were equally released under both

treatments (p-value > 0.05) in all experiments (Table S5). The humic-like C_{424} was not different among treatments in *P. angustum* and SOLA-spring and not detected in the balanced treatments for both *S. alaskensis* and SOLA-fall (Table S5).

The protein-like C_{340} showed a significant (p-value <0.01) and positive relationship to the growth rates under P-repletion (Fig. 4a) but this relationship was not evidenced under P-limitation (Fig. 4b). Conversely, the humic-like components C_{460} and C_{398} were negatively related to the growth rates in both treatments (p-value <0.01 and p-value <0.05 respectively). The other components were not significantly related to growth rates (Table S6).

Discussion

In this study, using 2 marine bacterial strains with contrasting lifestyles and 2 natural HP communities from different seasons, we showed that P-limitation influences the quality of HP-DOM, but not the net quantity released to the media. In addition, under P-replete conditions, the quality of the released FDOM was related to the growth rates.

Significant amounts of DOM were released in all experiments regardless of the nutrient condition, in line with previous studies showing that HP can be an important DOM source (Gruber et al., 2006; Koch et al., 2014; Ogawa, 2001; Ortega-Retuerta et al., 2021). Interestingly, DOM released by natural HP communities was lower than DOM released by the 2 single strains. This could be due to trophic cooperation in mixed communities (mainly SOLA-fall), i.e. DOM released by some taxa can be consumed by others within the community (Fritts et al., 2021). Contrary to the single strains, natural communities appeared to be less well adapted to efficiently uptake glucose (Table S4), also suggested by (Lønborg et al., 2019). We cannot exclude that in the mixed communities, viral lysis could contribute to some extent releasing back some glucose and monosaccharides to the media.

P-limitation did not induce an increase in the net HP-DOM released during our experiments. However, DOM release per biomass unit tended to be higher (although non-significant) in the unbalanced treatments in single strain experiments (Fig S3). In line with this, a previous study by Thompson & Cotner (2020) showed higher DOM release at high media C:P ratios (P-limitation) for bacteria with

249 strong internal elemental homeostasis. In the case of the mixed natural communities, this trend was not
250 clear especially since the HP-DOM release was much lower.
251 In the present study, growth efficiencies were also lower under P-limitation while the amount of glucose
252 consumed was similar between treatments in all experiments (Table S4). Since no significantly higher
253 DOM was released (although visible in some experiments, Fig S3), this suggests that under P-limitation
254 a higher proportion of the initial C-glucose was respired instead of being incorporated into biomass.
255 This is in line with previous studies showing an enhanced growth efficiency when P is available
256 (Guillemette & del Giorgio, 2012; Smith & Prairie, 2004). Together, these results suggest that the effect
257 of P-limitation on HP-DOM release is complex and could vary among microbial taxa depending on
258 their metabolic strategies or on the presence of cooperation processes in the case of mixed communities.
259 Even though HP-DOM quantity was similar among treatments, the FDOM fingerprints hint towards
260 different HP-DOM chemical composition driven by P (Fig. 3). The microbial humic-like fluorescence
261 (C_{398}), which increased in the P limited treatments of the strains and the natural community from fall,
262 has been used as a marker for microbially derived recalcitrant DOM in the ocean (Catalá et al., 2015;
263 Yamashita & Tanoue, 2008). Our results thus suggest that P-limitation promotes the release of more
264 presumably recalcitrant FDOM by HP. A possible explanation for this is the adaptation strategies of the
265 cells to P depletion. To reduce their P requirements, heterotrophic bacteria can substitute P-containing
266 lipids by P-free lipids in the cellular membrane (Chan et al., 2012; Sebastián et al., 2016). It has also
267 been observed that nutrient limitation, namely P, in the presence of excess glucose, leads to the
268 excretion of "overflow-metabolites'', i.e. intermediary metabolites resulting from alternative metabolic
269 pathways used to reduce the involvement of the limiting nutrient (Krämer, 1994; Neijssel & Tempest,
270 1975). We can speculate that the compounds released through these adaptive metabolic pathways have
271 a distinct fluorescence signature, likely similar to humic-like fluorescence.
272 Interestingly, the natural community from spring did not follow this trend. A different community
273 composition between seasons (Lambert et al., 2019) could explain this different response, since
274 different prokaryotic taxa have contrasting responses to P-limitation (Sebastián and Gasol 2013) .
275 In contrast, the protein-like fluorescence signal was generally higher under balanced growth and
276 decreased with P-limitation. In line with our result, Romano et al. (2014) showed that under P-surplus

conditions, peptides were one of the main secreted compounds by *Pseudovibrio* sp. FO-BEG1. However, this was not the case for *S. alaskensis*, showing overall a low protein-like signature that increased under P-limitation. *S. alaskensis*, a model oligotroph (Cavicchioli et al., 2003), presents low growth rates, while *P. angustum* and natural HP communities grew faster. As confirmed in our study, the release of protein-like FDOM under P-repletion is related to growth rates. This emphasizes the role of the different growth strategies between the considered HP, in agreement with (Weissman et al., 2021) who demonstrated that gene families involved in rapid protein production were overrepresented in genomes of fast-growing copiotrophs relative to slow-growing oligotrophs. In the other hand, growth rates did not significantly vary between conditions while protein-like fluorescence changed, indicating that growth rate is not the only predictor of protein-like release. Indeed, P-limitation also affects secondary metabolism of marine bacteria (e.g. Martín, 2004; Romano et al., 2015). This latter study (and references within) detected several proteins potentially involved in oxidative stress response and antibiotic production. It is likely that bacteria invest more in stress coping metabolism than in growth when P starved and this could explain the uncoupling of growth and protein-like FDOM release under P-limitation.

Conclusion

We could demonstrate that P-limitation plays an important role in HP-DOM release, leading to a relative increase in the likely recalcitrant (based on previous evidences) humic-like FDOM with a decrease in the presumably labile protein-like. We hypothesize that P availability would thus play an important role shaping the microbial carbon pump. Further work is needed to confirm the influence of P-limitation on the bioavailability of HP-derived DOM.

Acknowledgements

This work was supported by the Caramba (European commission, H2020-MSCA-IF-2015-703991), ODISEA (INSU LEFE/CYBER 2019) and MicroPump (ANR-20-CE01-0007) projects

304 to EOR. Flow cytometric analyses were performed at the BioPic cytometry and imaging platform
305 (Sorbonne University/CNRS). The authors thank the crew of R/V 'Nereis II' and the technicians of the
306 Banyuls observation service for their assistance in getting Mediterranean Sea samples, as well as Franck
307 Li, Cécile Carpaneto-Bastos and Lorenzo Scenna for their help with the SOLA-spring experiment.

References

Benner, R., & Strom, M. (1993). A critical evaluation of the analytical blank associated with DOC measurements by high-temperature catalytic oxidation. *Marine Chemistry*, *41*(1), 153–160. https://doi.org/10.1016/0304-4203(93)90113-3

Carlson, C. A. (2002). Chapter 4—Production and Removal Processes. In D. A. Hansell & C. A. Carlson (Eds.), *Biogeochemistry of Marine Dissolved Organic Matter* (pp. 91–151). Academic Press. https://doi.org/10.1016/B978-012323841-2/50006-3

Carlson, C., del Giorgio, P., & Herndl, G. (2007). Microbes and the Dissipation of Energy and Respiration: From Cells to Ecosystems. *Oceanography*, *20*(2), 89–100. https://doi.org/10.5670/oceanog.2007.52

Catalá, T. S., Reche, I., Fuentes-Lema, A., Romera-Castillo, C., Nieto-Cid, M., Ortega-Retuerta, E., Calvo, E., Álvarez, M., Marrasé, C., Stedmon, C. A., & Álvarez-Salgado, X. A. (2015). Turnover time of fluorescent dissolved organic matter in the dark global ocean. *Nature Communications*, *6*(1), 5986. https://doi.org/10.1038/ncomms6986

Cavicchioli, R., Ostrowski, M., Fegatella, F., Goodchild, A., & Guixa-Boixereu, N. (2003). Life under Nutrient Limitation in Oligotrophic Marine Environments: An Eco/Physiological Perspective of Sphingopyxis alaskensis (formerly Sphingomonas alaskensis). *Microbial Ecology*, *46*(2), 249–256. https://doi.org/10.1007/s00248-002-3008-6

Chan, L.-K., Newton, R., Sharma, S., Smith, C., Rayapati, P., Limardo, A., Meile, C., & Moran, M. A. (2012). Transcriptional Changes Underlying Elemental Stoichiometry Shifts in a Marine Heterotrophic Bacterium. *Frontiers in Microbiology*, *3*, 159. https://doi.org/10.3389/fmicb.2012.00159

Cole, J., Findlay, S., & Pace, M. (1988). Bacterial production in fresh and saltwater ecosystems: A cross-system overview. *Marine Ecology Progress Series*, *43*, 1–10. https://doi.org/10.3354/meps043001

Daoud, A. B. A., & Tremblay, L. (2019). HPLC-SEC-FTIR characterization of the dissolved organic matter produced by the microbial carbon pump. *Marine Chemistry*, *215*, 103668. https://doi.org/10.1016/j.marchem.2019.103668

del Giorgio, P. A., & Cole, J. J. (1998). Bacterial Growth Efficiency in Natural Aquatic Systems. *Annual Review of Ecology and Systematics*, *29*, 503–541.

Eguchi, M., Ostrowski, M., Fegatella, F., Bowman, J., Nichols, D., Nishino, T., & Cavicchioli, R. (2001). Sphingomonas alaskensis Strain AFO1, an Abundant Oligotrophic Ultramicrobacterium from the North Pacific. *Applied and Environmental Microbiology*, *67*(11), 4945–4954. https://doi.org/10.1128/AEM.67.11.4945-4954.2001

Fegatella, F., Lim, J., Kjelleberg, S., & Cavicchioli, R. (1998). Implications of rRNA operon copy number and ribosome content in the marine oligotrophic ultramicrobacterium Sphingomonas sp. Strain RB2256. *Applied and Environmental Microbiology*, *64*(11), 4433–4438. https://doi.org/10.1128/AEM.64.11.4433-4438.1998

Fritts, R. K., McCully, A. L., & McKinlay, J. B. (2021). Extracellular Metabolism Sets the Table for Microbial Cross-Feeding. *Microbiology and Molecular Biology Reviews*, *85*(1), e00135-20. https://doi.org/10.1128/MMBR.00135-20

Goldman, J. C., Caron, D. A., & Dennett, M. R. (1987). Regulation of gross growth efficiency and ammonium regeneration in bacteria by substrate C: N ratio1. *Limnology and Oceanography*, *32*(6), 1239–1252. https://doi.org/10.4319/lo.1987.32.6.1239

Goto, S., Tada, Y., Suzuki, K., & Yamashita, Y. (2020). Evaluation of the Production of Dissolved Organic Matter by Three Marine Bacterial Strains. *Frontiers in Microbiology*, *11*, 584419. https://doi.org/10.3389/fmicb.2020.584419

Gruber, D. F., Simjouw, J.-P., Seitzinger, S. P., & Taghon, G. L. (2006). Dynamics and Characterization of Refractory Dissolved Organic Matter Produced by a Pure Bacterial Culture in an Experimental Predator-Prey System. *Applied and Environmental Microbiology*, *72*(6), 4184–4191. https://doi.org/10.1128/AEM.02882-05

Guillemette, F., & del Giorgio, P. A. (2012). Simultaneous consumption and production of fluorescent dissolved organic matter by lake bacterioplankton. *Environmental Microbiology*, *14*(6), 1432–1443. https://doi.org/10.1111/j.1462-2920.2012.02728.x

Hansell, D. A. (2013). Recalcitrant Dissolved Organic Carbon Fractions. *Annual Review of Marine Science*, *5*(1), 421–445. https://doi.org/10.1146/annurev-marine-120710-100757

Heinrichs, M. E., Heyerhoff, B., Arslan-Gatz, B. S., Seidel, M., Niggemann, J., & Engelen, B. (2022). Deciphering the Virus Signal Within the Marine Dissolved Organic Matter Pool. *Frontiers in Microbiology*, *13*, 863686. https://doi.org/10.3389/fmicb.2022.863686

Hopkinson, C. S., & Vallino, J. J. (2005). Efficient export of carbon to the deep ocean through dissolved organic matter. *Nature*, *433*, 142–145. https://doi.org/10.1038/nature03191

Jiao, N., Herndl, G. J., Hansell, D. A., Benner, R., Kattner, G., Wilhelm, S. W., Kirchman, D. L., Weinbauer, M. G., Luo, T., Chen, F., & Azam, F. (2010). Microbial production of

recalcitrant dissolved organic matter: Long-term carbon storage in the global ocean. *Nature Reviews Microbiology*, *8*(8), 593–599. https://doi.org/10.1038/nrmicro2386

Kawasaki, N., & Benner, R. (2006). Bacterial release of dissolved organic matter during cell growth and decline: Molecular origin and composition. *Limnology and Oceanography*, *51*(5), 2170–2180. https://doi.org/10.4319/lo.2006.51.5.2170

Koch, B. P., Kattner, G., Witt, M., & Passow, U. (2014). Molecular insights into the microbial formation of marine dissolved organic matter: Recalcitrant or labile? *Biogeosciences*, *11*(15), 4173–4190. https://doi.org/10.5194/bg-11-4173-2014

Koedooder, C., Guéneuguès, A., Van Geersdaële, R., Vergé, V., Bouget, F.-Y., Labreuche, Y., Obernosterer, I., & Blain, S. (2018). The Role of the Glyoxylate Shunt in the Acclimation to Iron Limitation in Marine Heterotrophic Bacteria. *Frontiers in Marine Science*, *5*, 435. https://doi.org/10.3389/fmars.2018.00435

Kramer, G., & Herndl, G. (2004). Photo- and bioreactivity of chromophoric dissolved organic matter produced by marine bacterioplankton. *Aquatic Microbial Ecology*, *36*, 239–246. https://doi.org/10.3354/ame036239

Krämer, R. (1994). Secretion of amino acids by bacteria: Physiology and mechanism. *FEMS Microbiology Reviews*, *13*(1), 75–93. https://doi.org/10.1111/j.1574-6976.1994.tb00036.x

Kujawinski, E. B. (2011). The Impact of Microbial Metabolism on Marine Dissolved Organic Matter. *Annual Review of Marine Science*, *3*(1), 567–599. https://doi.org/10.1146/annurev-marine-120308-081003

Lambert, S., Tragin, M., Lozano, J.-C., Ghiglione, J.-F., Vaulot, D., Bouget, F.-Y., & Galand, P. E. (2019). Rhythmicity of coastal marine picoeukaryotes, bacteria and archaea

despite irregular environmental perturbations. *The ISME Journal*, *13*(2), 388–401. https://doi.org/10.1038/s41396-018-0281-z

Lauro, F. M., McDougald, D., Thomas, T., Williams, T. J., Egan, S., Rice, S., DeMaere, M. Z., Ting, L., Ertan, H., Johnson, J., Ferriera, S., Lapidus, A., Anderson, I., Kyrpides, N., Munk, A. C., Detter, C., Han, C. S., Brown, M. V., Robb, F. T., … Cavicchioli, R. (2009). The genomic basis of trophic strategy in marine bacteria. *Proceedings of the National Academy of Sciences*, *106*(37), 15527–15533. https://doi.org/10.1073/pnas.0903507106

Lazzari, P., Solidoro, C., Salon, S., & Bolzon, G. (2016). Spatial variability of phosphate and nitrate in the Mediterranean Sea: A modeling approach. *Deep Sea Research Part I: Oceanographic Research Papers*, *108*, 39–52. https://doi.org/10.1016/j.dsr.2015.12.006

Lê, S., Josse, J., & Husson, F. (2008). FactoMineR: An R Package for Multivariate Analysis. *Journal of Statistical Software*, *25*, 1–18. https://doi.org/10.18637/jss.v025.i01

Lechtenfeld, O. J., Hertkorn, N., Shen, Y., Witt, M., & Benner, R. (2015). Marine sequestration of carbon in bacterial metabolites. *Nature Communications*, *6*(1), 6711. https://doi.org/10.1038/ncomms7711

Lønborg, C., Álvarez-Salgado, X. A., Davidson, K., & Miller, A. E. J. (2009). Production of bioavailable and refractory dissolved organic matter by coastal heterotrophic microbial populations. *Estuarine, Coastal and Shelf Science*, *82*(4), 682–688. https://doi.org/10.1016/j.ecss.2009.02.026

Lønborg, C., Baltar, F., Carreira, C., & Morán, X. A. G. (2019). Dissolved Organic Carbon Source Influences Tropical Coastal Heterotrophic Bacterioplankton Response to

Experimental Warming. *Frontiers in Microbiology*, *10*. https://www.frontiersin.org/articles/10.3389/fmicb.2019.02807

Martín, J. F. (2004). Phosphate Control of the Biosynthesis of Antibiotics and Other Secondary Metabolites Is Mediated by the PhoR-PhoP System: An Unfinished Story. *Journal of Bacteriology*, *186*(16), 5197–5201. https://doi.org/10.1128/JB.186.16.5197-5201.2004

Matallana-Surget, S., Joux, F., Wattiez, R., & Lebaron, P. (2012). Proteome Analysis of the UVB-Resistant Marine Bacterium Photobacterium angustum S14. *PLoS ONE*, *7*(8), e42299. https://doi.org/10.1371/journal.pone.0042299

Middelboe, M., & Jørgensen, N. O. G. (2006). Viral lysis of bacteria: An important source of dissolved amino acids and cell wall compounds. *Journal of the Marine Biological Association of the United Kingdom*, *86*(3), 605–612. https://doi.org/10.1017/S0025315406013518

Murphy, K. R., Stedmon, C. A., Graeber, D., & Bro, R. (2013). Fluorescence spectroscopy and multi-way techniques. PARAFAC. *Analytical Methods*, *5*(23), 6557–6566. https://doi.org/10.1039/C3AY41160E

Myklestad, S. M., Skånøy, E., & Hestmann, S. (1997). A sensitive and rapid method for analysis of dissolved mono- and polysaccharides in seawater. *Marine Chemistry*, *56*(3), 279–286. https://doi.org/10.1016/S0304-4203(96)00074-6

Nagata, T. (2000). Production mechanisms of dissolved organic matter. *Microbial Ecology of the Oceans*. https://cir.nii.ac.jp/crid/1572543025403471744

Nagata, T. (2008). Organic Matter–Bacteria Interactions in Seawater. In D. L. Kirchman (Ed.), *Microbial Ecology of the Oceans* (pp. 207–241). John Wiley & Sons, Inc. https://doi.org/10.1002/9780470281840.ch7

Neijssel, O. M., & Tempest, D. W. (1975). The regulation of carbohydrate metabolism in Klebsiella aerogenes NCTC 418 organisms, growing in chemostat culture. *Archives of Microbiology*, *106*(3), 251–258. https://doi.org/10.1007/BF00446531

Obernosterer, I., Kawasaki, N., & Benner, R. (2003). P-limitation of respiration in the Sargasso Sea and uncoupling of bacteria from P-regeneration in size-fractionation experiments. *Aquatic Microbial Ecology*, *32*(3), 229–237. https://doi.org/10.3354/ame032229

Ogawa, H. (2001). Production of Refractory Dissolved Organic Matter by Bacteria. *Science*, *292*(5518), 917–920. https://doi.org/10.1126/science.1057627

Ortega-Retuerta, E., Devresse, Q., Caparros, J., Marie, B., Crispi, O., Catala, P., Joux, F., & Obernosterer, I. (2021). Dissolved organic matter released by two marine heterotrophic bacterial strains and its bioavailability for natural prokaryotic communities. *Environmental Microbiology*, *23*(3), 1363–1378. https://doi.org/10.1111/1462-2920.15306

Osterholz, H., Niggemann, J., Giebel, H.-A., Simon, M., & Dittmar, T. (2015). Inefficient microbial production of refractory dissolved organic matter in the ocean. *Nature Communications*, *6*(1), 7422. https://doi.org/10.1038/ncomms8422

Rochelle-Newall, E. J., & Fisher, T. R. (2002). Production of chromophoric dissolved organic matter fluorescence in marine and estuarine environments: An investigation into the role of phytoplankton. *Marine Chemistry*, *77*(1), 7–21. https://doi.org/10.1016/S0304-4203(01)00072-X

Romano, S., Dittmar, T., Bondarev, V., Weber, R. J. M., Viant, M. R., & Schulz-Vogt, H. N. (2014). Exo-Metabolome of Pseudovibrio sp. FO-BEG1 Analyzed by Ultra-High

Resolution Mass Spectrometry and the Effect of Phosphate Limitation. *PLoS ONE*, *9*(5), e96038. https://doi.org/10.1371/journal.pone.0096038

Romano, S., Schulz-Vogt, H. N., González, J. M., & Bondarev, V. (2015). Phosphate Limitation Induces Drastic Physiological Changes, Virulence-Related Gene Expression, and Secondary Metabolite Production in Pseudovibrio sp. Strain FO-BEG1. *Applied and Environmental Microbiology*, *81*(10), 3518–3528. https://doi.org/10.1128/AEM.04167-14

Schut, F., de Vries, E. J., Gottschal, J. C., Robertson, B. R., Harder, W., Prins, R. A., & Button, D. K. (1993). Isolation of Typical Marine Bacteria by Dilution Culture: Growth, Maintenance, and Characteristics of Isolates under Laboratory Conditions. *Applied and Environmental Microbiology*, *59*(7), 2150–2160. https://doi.org/10.1128/aem.59.7.2150-2160.1993

Sebastián, M., & Gasol, J. M. (2013). Heterogeneity in the nutrient limitation of different bacterioplankton groups in the Eastern Mediterranean Sea. *The ISME Journal*, *7*(8), 1665–1668. https://doi.org/10.1038/ismej.2013.42

Sebastián, M., Smith, A. F., González, J. M., Fredricks, H. F., Van Mooy, B., Koblížek, M., Brandsma, J., Koster, G., Mestre, M., Mostajir, B., Pitta, P., Postle, A. D., Sánchez, P., Gasol, J. M., Scanlan, D. J., & Chen, Y. (2016). Lipid remodelling is a widespread strategy in marine heterotrophic bacteria upon phosphorus deficiency. *The ISME Journal*, *10*(4), 968–978. https://doi.org/10.1038/ismej.2015.172

Shimotori, K., Omori, Y., & Hama, T. (2009). Bacterial production of marine humic-like fluorescent dissolved organic matter and its biogeochemical importance. *Aquatic Microbial Ecology*, *58*, 55–66. https://doi.org/10.3354/ame01350

Shimotori, K., Watanabe, K., & Hama, T. (2012). Fluorescence characteristics of humic-like fluorescent dissolved organic matter produced by various taxa of marine bacteria. *Aquatic Microbial Ecology*, *65*(3), 249–260. https://doi.org/10.3354/ame01552

Smith, E. M., & Prairie, Y. T. (2004). Bacterial metabolism and growth efficiency in lakes: The importance of phosphorus availability. *Limnology and Oceanography*, *49*(1), 137–147. https://doi.org/10.4319/lo.2004.49.1.0137

Thompson, S. K., & Cotner, J. B. (2020). P-limitation drives changes in DOM production by aquatic bacteria. *Aquatic Microbial Ecology*, *85*, 35–46. https://doi.org/10.3354/ame01940

Weissman, J. L., Hou, S., & Fuhrman, J. A. (2021). Estimating maximal microbial growth rates from cultures, metagenomes, and single cells via codon usage patterns. *Proceedings of the National Academy of Sciences*, *118*(12), e2016810118. https://doi.org/10.1073/pnas.2016810118

Wu, J., Sunda, W., Boyle, E. A., & Karl, D. M. (2000). Phosphate Depletion in the Western North Atlantic Ocean. *Science*. https://doi.org/10.1126/science.289.5480.759

Yamashita, Y., & Tanoue, E. (2008). Production of bio-refractory fluorescent dissolved organic matter in the ocean interior. *Nature Geoscience*, *1*(9), 579–582. https://doi.org/10.1038/ngeo279

Tables

Table 1 *Growth parameters and DOM quantification in all experiments: Prokaryotic growth efficiency PGE (mean ± standard deviation), growth rate (mean ± standard deviation), heterotrophic prokaryotic DOM (HP-DOM) net quantity (mean ± standard deviation), percentage of initial C-glucose released as HP-DOM. Letters indicate significant differences, n.d. = non-determined.*

Figures

Fig. 1 *Changes in cell abundance in P. angustum (a), S. alaskensis (b), SOLA-fall (c), and SOLA-spring (d) experiments. Dots represent the experimental replicates and lines represent mean cell abundances. Note the different scales for x and y axes.*

Fig. 2 *Biplot of the first 2 axes of correspondence analysis (CA) performed on the PARAFAC components, each dot representing an experimental replicate (See material and methods and Supporting information for details on replicates).* C_{340}*: protein-like;* C_{460}*: fulvic like;* C_{354}*: protein-/phenolic-like;* C_{398}*: microbial humic-like;* C_{440}*: terrestrial humic-like;* C_{424}*: humic-like.*

Fig. 3 *FDOM characterisation at* T_f*: EEMs contour plots at* T_f *(only one out of the replicates is shown) (a). Red labels show modelled component location, only primary excitation peak is considered. Note the difference in colormap scale. FDOM Maximum fluorescence intensities of Protein-like* C_{340} *component (c) and microbial humic-like* C_{398} *component (d) at* T_f *in the different experimental treatments. Dots represent replicates (See material and methods and Supporting information for details on replicates).*

Fig. 4 Linear regression between the protein-like component C_{340} *and growth rate in (a) balanced treatment and (b) unbalanced treatment. Dots represent replicates (See material and methods and Supporting information for details on replicates).*

Tables

Table 2 *Growth parameters and DOM quantification in all experiments: Prokaryotic growth efficiency PGE (mean ± standard deviation), growth rate (mean ± standard deviation), heterotrophic prokaryotic DOM (HP-DOM) net quantity (mean ± standard deviation), percentage of initial C-glucose released as HP-DOM. Letters indicate significant differences, n.d. = non-determined.*

Experiment-Treatment	*Growth rate (h^{-1})*	*PGE (%)*	*HP-DOM (µmol L^{-1})*	*% to initial C-Glucose*
P. angustum				
Balanced	0.480 ± 0.039 [a]	21.94 ± 0.27 [a]	50.5 ± 18.3 [a]	21 ± 7%
Unbalanced	0.418 ± 0.042 [a]	16.15 ± 0.31 [b]	60.2 ± 44.9 [a]	30 ± 23%
S. alaskensis				
Balanced	0.093 ± 0.002 [a]	34.82 ± 1.64 [a]	52.4 ± 8.1[a]	28 ± 4%
Unbalanced	0.085 ± 0.003 [a]	12.02 ± 0.69 [b]	52.1 ± 13.8 [a]	23 ± 6%
SOLA-fall				
Balanced	0.500 ± 0.035 [a]	23.06 ± 3.53[a]	18.2 ± 4.8 [a]	10 ± 3%
Unbalanced	0.475 ± 0.028 [a]	9.19 ± 0.18 [b]	5.3 ± 5.5 [a]	3 ± 3%
SOLA-spring				
Balanced	0.221 ± 0.08 [a]	10.51 ± 3.22 [a]	43.2 ± 15.5	18 ± 7%
Unbalanced	0.179 ± 0.097 [a]	4.04 ± 0.20 [b]	n.d.	n.d.

Figures

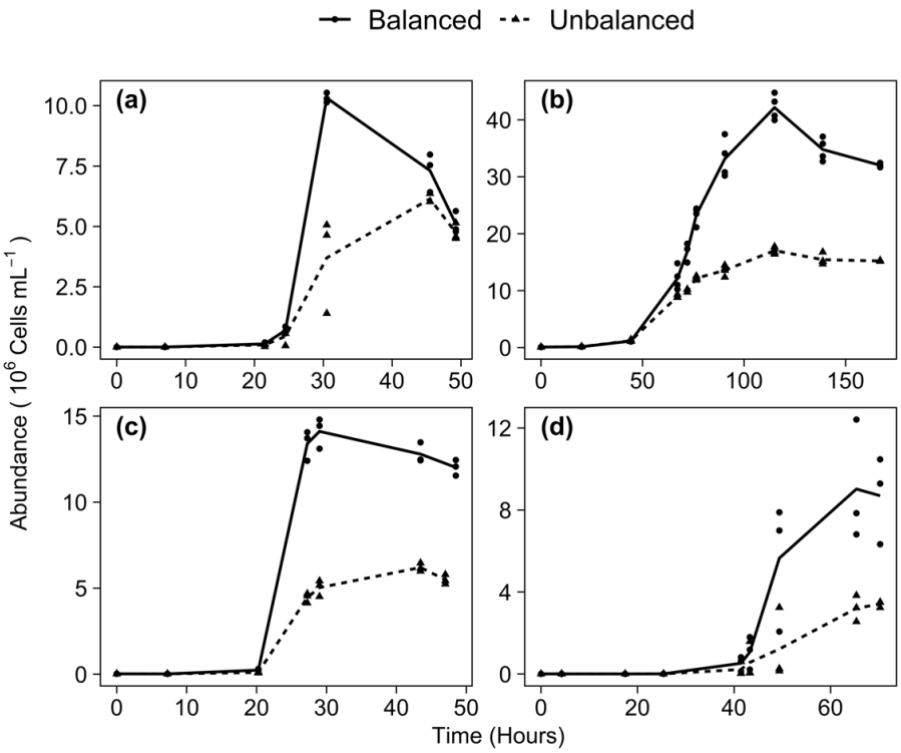

Fig. 5 *Changes in cell abundance in P. angustum (a), S. alaskensis (b), SOLA-fall (c), and SOLA-spring (d) experiments. Dots represent the experimental replicates and lines represent mean cell abundances. Note the different scales for x and y axes.*

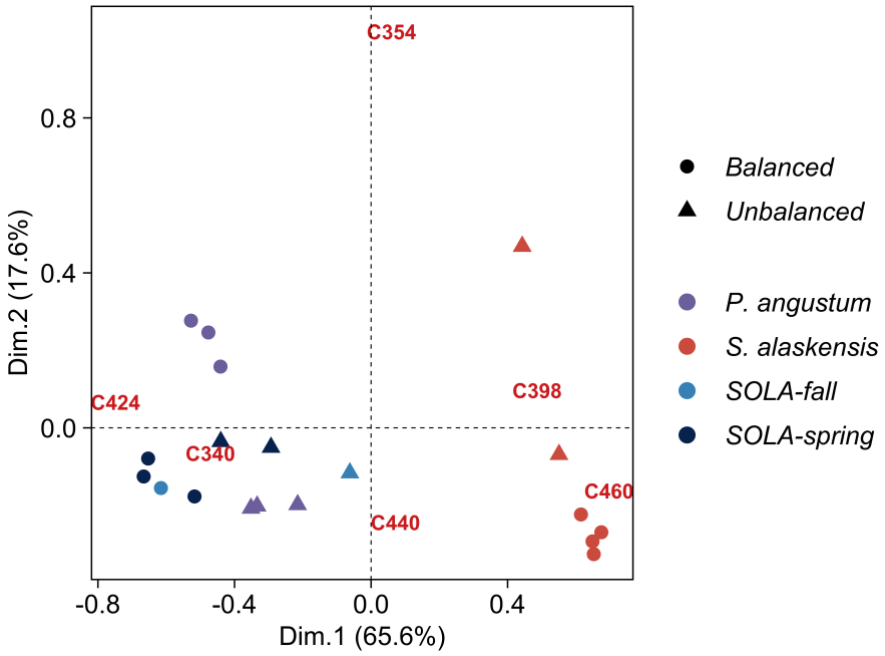

Fig. 6 *Biplot of the first 2 axes of correspondence analysis (CA) performed on the PARAFAC components, each dot representing an experimental replicate (See material and methods and Supporting information for details on replicates). C_{340}: protein-like; C_{460}: fulvic like; C_{354}: protein-/phenolic-like; C_{398}: microbial humic-like; C_{440}: terrestrial humic-like; C_{424}: humic-like.*

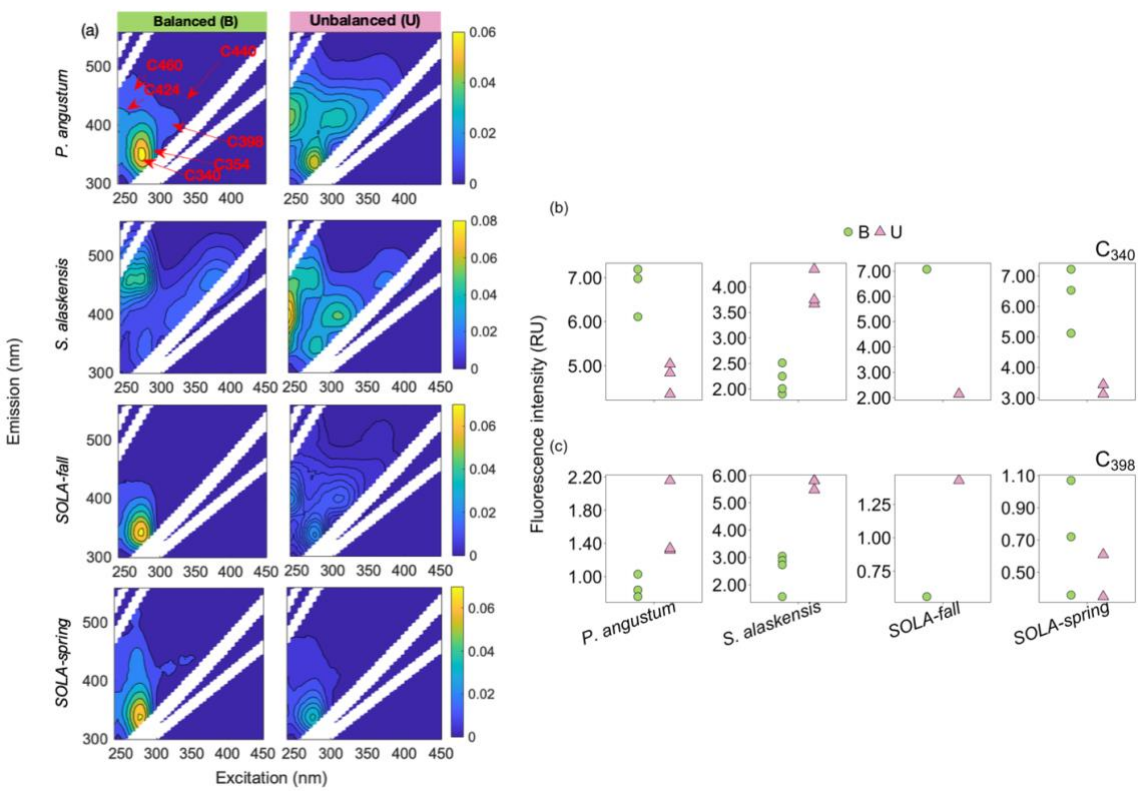

Fig. 7 *FDOM characterisation at T_f: EEMs contour plots at T_f (only one out of the replicates is shown) (a). Red labels show modelled component location, only primary excitation peak is considered. Note the difference in colormap scale. FDOM Maximum fluorescence intensities of Protein-like C_{340} component (c) and microbial humic-like C_{398} component (d) at T_f in the different experimental treatments. Dots represent replicates (See material and methods and Supporting information for details on replicates).*

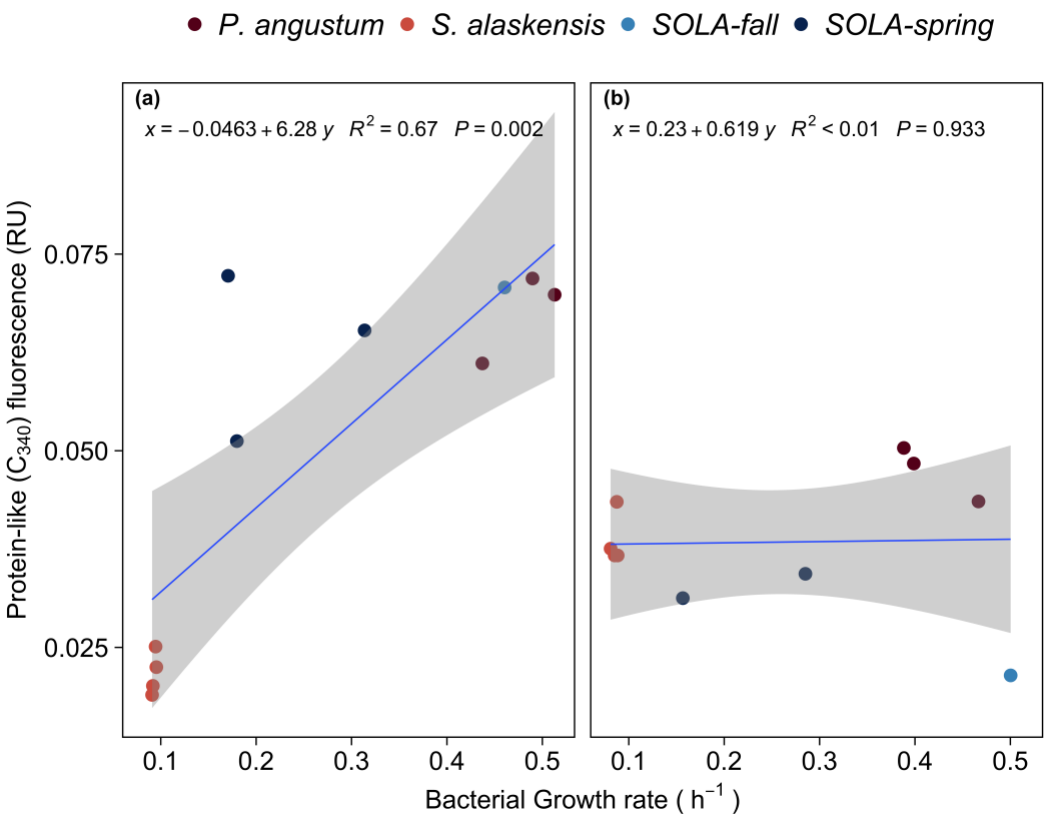

Fig. 8 *Linear regression between the protein-like component C340 and growth rate in (a) balanced treatment and (b) unbalanced treatment. Dots represent replicates (See material and methods and Supporting information for details on replicates).*

Supporting Information

Supplementary material and methods

Heterotrophic prokaryotes abundance

HP growth was followed by flow cytometry using a Beckman CytoFLEX bench instrument. 500 µL samples were fixed with glutaraldehyde (0.5 % final concentration) and preserved at -80 °C prior to analysis. Just before analysis samples were thawed and stained with SYBR Green (0.025% (v/v) final concentration) and fluorescent beads (1µm) were added as an internal standard. Samples were run at medium speed (30 µL.min^{-1}) for 60 seconds. Prokaryotes were identified in plots of side scatter (SSC) vs. green florescence (FITC).

Chemical analyses

Samples for dissolved organic carbon (DOC) concentration were taken into 10 mL pre-combusted glass ampoules, acidified with 85 % H_3PO_4 to pH=2. The ampoules were flame-sealed and stored in the dark at room temperature until analysis. DOC was analyzed using the high temperature catalytic oxidation technique with a Shimadzu TOC-L analyzer (Benner and Strom 1993). Calibration curves were made using an acetanilide solution (C_8H_9NO) and deep seawater standards (44–45 µmol C L^{-1}), provided by the Consensus Reference Material Hansell program (Univ. of Miami), were used to assess the accuracy of the measurements.

Samples (200 µL) for dissolved glucose were stored in pre-combusted glass vials at -20 °C until analysis. Glucose quantification was done based on an adapted colorimetric protocol from Myklestad et al. (1997). The reagents were calibrated daily using a standard curve made of D-Glucose. MilliQ water and artificial sea water blanks were ran in triplicate before and after each batch of samples. Glucose concentrations were expressed as µmol L^{-1} of carbon equivalent (C-glucose). This approach detects not only glucose but also other dissolved monosaccharides.

Samples for inorganic nutrients (11 ml, NO_3^-, NO_2^-, and PO_4^{3-}) were stored at -20 °C until analysis. Quantification was done using segmented flow analyzer (Bran+Luebbe) with colorimetric detection

using methods described in Aminot and Kérouel (2007). The accuracy of the method was assessed using reference material (Certipur, Merck). The precisions were in the range of 1–4%, and the detection limits were 0.02 µmol L^{-1} for NO_3^- , 0.01 µmol L^{-1} for NO_2^- and PO_4^{3-}. NH_4^+ (7 mL) samples were collected into pre-rinsed tubes and analyzed freshly by fluorometry using a DeNovix QFX Fluorometer.

FDOM measurements

In addition to the EEMs, 5 discrete excitation emission pairs were measured as described in (Coble, 2007), in all of the experimental replicates. These excitation emission pairs are: 280 nm/350 nm (peak T) and 275 nm/310 nm (peak B) for tryptophan and tyrosine–like substances respectively; 250 nm/435 nm (peak A) for humic substances of different origins; 340 nm/440 nm (peak C) for terrestrial humic-like; 320 nm/410 nm (peak M) for marine humic-like substances. In SOLA-fall experiment, we recorded an EEM in only one randomly chosen replicate per treatment due to time constraints. In this experiment, fluorescence measurements of the 5 discrete excitation and emission pairs showed differences between triplicates from 0.1 to 16 %.

PARAFAC analysis method details

The data set used for PARAFAC modeling consisted of 113 EEMs, including 42 samples from the HP-DOM release experiments, of which 21 were measured during the exponential growth phase (data not shown), and 71 samples from HP-DOM degradation experiments conducted using the same HP-DOM (data not shown). T_0 samples were not included (very low fluorescent signal, Fig S1).

Raman and Rayleigh scattering bands were excised from all the dataset and replaced with missing values. Several models of 2-8 components were then fitted with a non-negative constraint using 'outliertest' function (drEEM Toolbox) in order to detect outlier samples and/or wavelengths. At this step, noisy measurements at excitation 240 nm were removed from all EEMs, and one replicate from SOLA-spring experiment (unbalanced treatment) was detected as an outlier and excluded. Based on these preliminary models' spectral properties, residuals and errors, the 6-component model was determined to be the best fit for this dataset and explained 99.3% of the variance. A final 6-component

model was computed out of 50 random initializations with a convergence criterion of 10^{-8}. The model was then split-half validated by dividing the dataset into 2 randomly selected halves as described by (Murphy et al. 2013). All model's components matched in all the splits with a Tucker Congruence Coefficient (TCC) > 0.95 in the excitation and emission loadings. The final model was compared to previously developed fluorescence DOM models on the OpenFluor database (Murphy et al. 2014). The number of matches was restricted to a threshold of TCC > 0.96 for excitation and TCC > 0.97 for emissions. All the components yielded several matching models allowing to describe their properties (Table S3).

Supplementary tables

Table S3 *Minimum media composition*

Salt	Final concentration (g L^{-1})
NaCl	24
Na_2SO_4	4
KCl	0.68
KBr	0.1
H_3BO_3	0.025
NaF	0.002
$MgCl_2.H_2O$	10.8
$CaCl_2$	1.5
$SrCl_2$	0.024
$NaHCO_3$	0.2
Metal	**Final concentration (µg L^{-1})**
$CuCl_2.H_2O$	15 x 10^{-3}
$NiCl_2.H_2O$	25 x 10^{-3}
$NaMOO_4.2H_2O$	25 x 10^{-3}
$ZnSO_4.7H_2O$	70 x 10^{-3}
$MnCl_2.4H_2O$	100 x 10^{-3}
$CoCl_2.6H_2O$	120 x 10^{-3}
FeEDTA	0.068 µM C
Vitamins	**Final concentration (nmol C L^{-1})**
P-aminobenzoic acid	2.6
D-biotin	0.8
Folic Acid	1
D-pantothenic acid	2.5
Pyridoxal	0.9
Pyridoxamine	4.8
Pyridoxine	5.2
Riboflavin	2.4
Thiamine	0.9
D L-6,8-thioctic acid	1
Vitamin B12	2.8
Nicotinamide	3.2

Table S4 Biomass conversion factors used for prokaryotes growth efficiencies calculation. Conversion factors were chosen to account for the differences in cell size and life styles. For *S. alaskensis* the fgC $Cell^{-1}$ was obtained by converting fgC μm^{-3} to fgC $Cell^{-1}$ considering a cell volume of 0.05 μm^3 (Eguchi et al. 2001) and a volume to C content conversion factor of 380 fgC μm^{-3} (Lee and Fuhrman 1987). We chose a higher conversion factor for the copiotrophic *P. angustum* based on a Vibrio C content estimate (Fagerbakke et al. 1996). Since our natural communities come from coastal water, we used the conversion factor for coastal bacteria reported in literature (Fukuda et. al. 1998).

Strain	Conversion factor	Reference
P. angustum	62 fgC $Cell^{-1}$	(Fagerbakke et al. 1996)
SOLA-fall SOLA-spring	30.2 fgC $Cell^{-1}$	(Fukuda et al. 1998)
S. alaskensis	19 fgC $Cell^{-1}$	(Lee and Fuhrman 1987; Eguchi et al. 2001)

Table S3 *Characteristics of the six components identified by PARAFAC analysis, ex = excitation and em = emission, examples of matching models for external validation and components classification into known florescence types.*

Component	Ex	Em	Examples of matching PARAFC models build in marine or freshwater systems (OpenFluor)		Fluorescence type classification	Classification reference
			Component ex/em	Source and Reference		
C_{340}	275	340	C1 275/342 C6 275/334	Coastal (Brym et al. 2014); Boreal lakes (Lapierre and del Giorgio 2014)	Protein-like (Tryptophan-like)	(Coble 2007; Stedmon and Markager 2005)
C_{460}	270 (385)	460	C2 270(380)/476 C5 260(385)/460	Estuary (Bittar et al. 2016); River (Gonçalves-Araujo et al. 2015)	Fulvic-like and humic-like	(Coble 2007)
C_{354}	290	354	C6 240/350 C4 248/355	Streams (Osburn et al. 2018); Lake (Catalá et al. 2016)	Protein- or phenolic-like related to processed humic-like material	(Catalán et al. 2021)
C_{398}	315	398	C3 240(310)/403	Estuary (Wang et al. 2020);	Marine/Microbial humic-like	(Yamashita et al. 2008; Coble 2007)
C_{440}	340(265)	440	C3 350/428	Waste water* (Murphy et al. 2011)	Terrestrial humic-like (C)	(Coble 2007)
C_{424}	250	424	C1 275/424 C1 250 (295)/412	Boreal lakes (Lapierre and del Giorgio 2014) Lake (Du et al. 2016)	Humic-like from diverse origins (A)	(Coble 2007)

* *Only one matching model*

Table S4 *Initial and final C-glucose and inorganic nutrient concentrations (mean ± standard deviation), percentage of C-glucose consumed and final DOC concentrations (mean ± standard deviation) in the different treatments (B = Balanced, U= Unbalanced), n.d.=not determined.*

Experiment-Treatment	C-glucose µmol L^{-1}		NH_4^+ µmol L^{-1}		PO_4^{3-} µmol L^{-1}		C-glucose consumption (%)	DOC µmol L^{-1}	
	T_0	T_f	T_0	T_f	T_0	T_f		T_0	T_f
P. angustum									
B	242.6	2.8±3.2	35.3	19.8±0.7	4.51	2.16±0.03	99.1	218.7	52.6 ±14.1
U	197.9	4.3±1.3	33.4	23.6±0.4	0.91	0.31±0.40	97.8	221.9	64.6 ±45.0
S. alaskensis									
B	185.1	1.8±1.7	30.1	8.8±0.6	4.49	2.84±0.11	99.0	247.5	53.2±5.2
U	223.9	9.4±9.2	32.8	12.0±0.5	0.68	0.18±0.21	95.8	271.5	57.7±6.7
SOLA-fall									
B	174.6	12.5±18.3	35.2	21.1±1.0	4.51	1.87±0.17	92.8	164.9	18.2±1.0
U	200.4	23.4±3.0	36.0	24.8±0.8	0.59	0.06±0.03	88.3	162	28.6±1.3
SOLA-spring									
B	245.9	18.2±5.4	31.6	16.6±0.9	4.27	2.20±0.16	92.6	214.8	61.4 ±19.0
U	247.5	22.5±5.3	32.7	21.4±0.4	0.63	0.06±0.03	90.9	224.5	n.d.*

* *Two out of 3 replicates showed unexpected values (> 200 µmol L^{-1}) and suspected to be DOC contaminated and thus* ***SOLA-spring*** *U DOC values were not considered.*

Table S5 *Maximum fluorescence intensities of all components at Tf in the different treatments (B = Balanced, U= Unbalanced). Values are expressed in (x10^{-2} RU)*

Experiment-Condition	C_{340}	C_{460}	C_{354}	C_{398}	C_{440}	C_{424}
P. angustum						
B	6.76 ± 0.57[a]	0.86[a] ± 0.33	1.27 ± 0.14[a]	0.88[a] ± 0.14	0.75 ± 0.36[a]	1.15 ± 0.47[a]
U	4.74 ± 0.35[b]	0.89[a] ± 0.40	0.00 ± 0.00[a]	1.60[a] ± 0.48	0.96 ± 0.65[a]	0.76 ± 0.87[a]
S. alaskensis						
B	2.17 ± 0.27[a]	4.50[a] ± 0.16	0.11 ± 0.08[a]	2.56[a] ± 0.67	1.02 ± 0.11[a]	0.00 ± 0.00[a]
U	3.86 ± 0.33[b]	4.24[a] ± 0.38	10.63 ± 17.49[a]	5.65[b] ± 0.20	0.84 ± 0.10[a]	0.18 ± 0.15[a]
SOLA-fall						
B	7.08 ± n.d	0.45[a] ± n.d	0.20 ± n.d	0.56 ± n.d	0.29 ± n.d	0.00 ± n.d
U	2.14 ± n.d	0.53[a] ± n.d	0.01 ± n.d	1.43 ± n.d	0.37 ± n.d	0.31 ± n.d
SOLA-spring						
B	6.29 ± 1.07[a]	0.53[a] ± 0.58	0.19 ± 0.16[a]	0.72[a] ± 0.36	0.55 ± 0.28[a]	0.89 ± 0.34[a]
U	3.28 ± 0.22[b]	0.59[a] ± 0.10	0.28 ± 0.02[a]	0.48[a] ± 0.19	0.37 ± 0.07[a]	0.15 ± 0.03[a]

Table S6 *Results of linear regression analysis between maximum fluorescence of the different FDOM components and growth rate in the different experimental treatments (B = Balanced, U= Unbalanced).*

Component	Treatment	Equation	p-value	r^2
C_{460}	B	*y = 0.4 – 6.7 x*	**0.009**	0.55
	U	*y = 0.4 – 7.6 x*	**0.005**	0.65
C_{354}	B	*y = 0.2 + 26.6 x*	**0.003**	0.65
	U	*y = 0.3 – 0.6 x*	0.3	0.16
C_{398}	B	*y = 0.4 – 12.0 x*	**0.02**	0.46
	U	*y = 0.4 – 5.4 x*	**0.02**	0.53
C_{440}	B	*y = 0.4 – 23.5 x*	0.2	0.19
	U	*y = 0.2 + 1.6 x*	0.9	0.0013
C_{424}	B	*y = 0. 2 + 16.9 x*	0.06	0.33
	U	*y = 0.2 + 17.2 x*	0.1	0.25

Supplementary figures

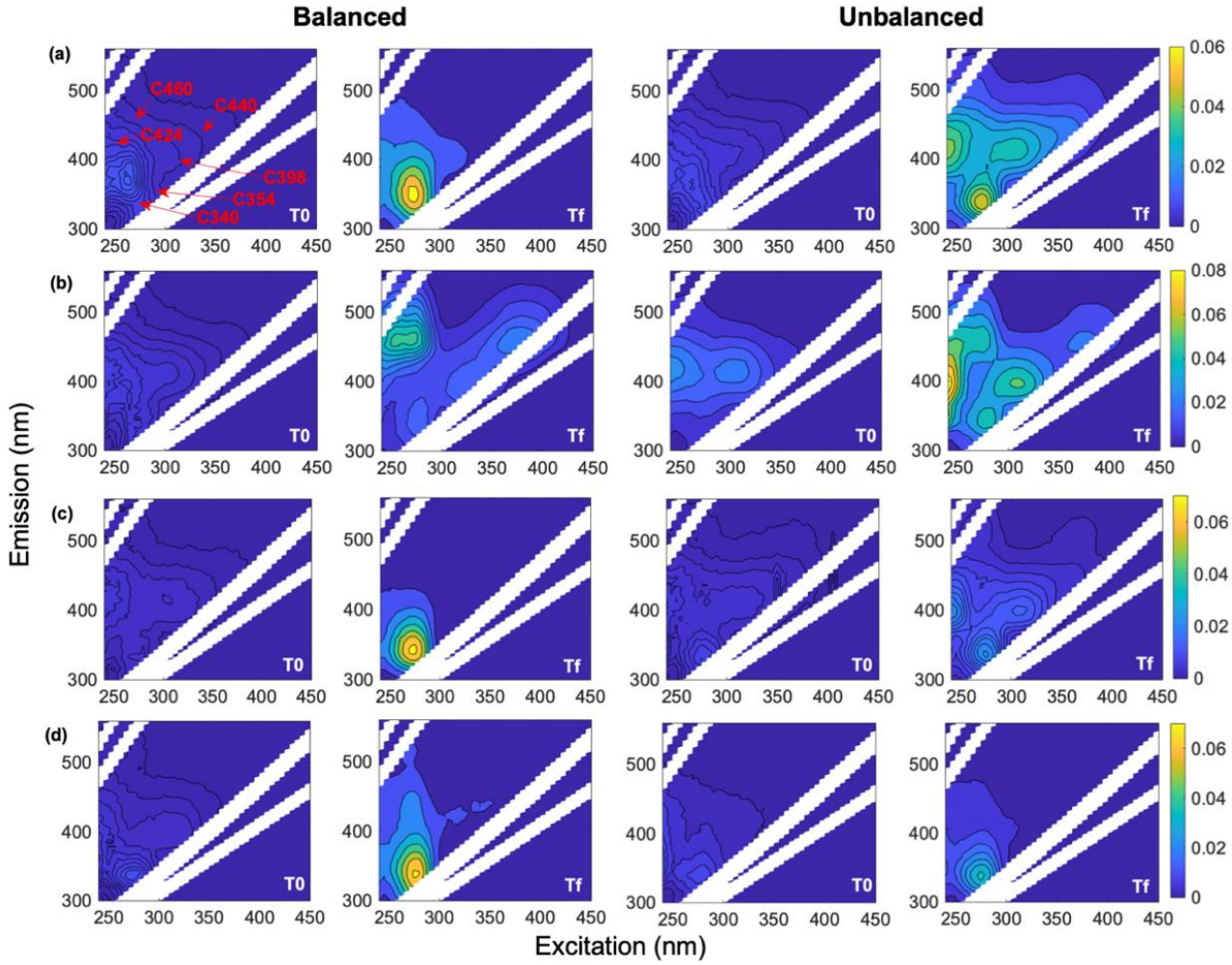

Fig S1 *EEMs contour plots at T_0 and T_f (only one out of the replicates is shown): (a) P. angustum, (b) S. alaskensis, (c) SOLA-fall, (d) SOLA-spring. Red labels show modelled component location, only primary excitation peak is considered. Note the difference in colormap scale.*

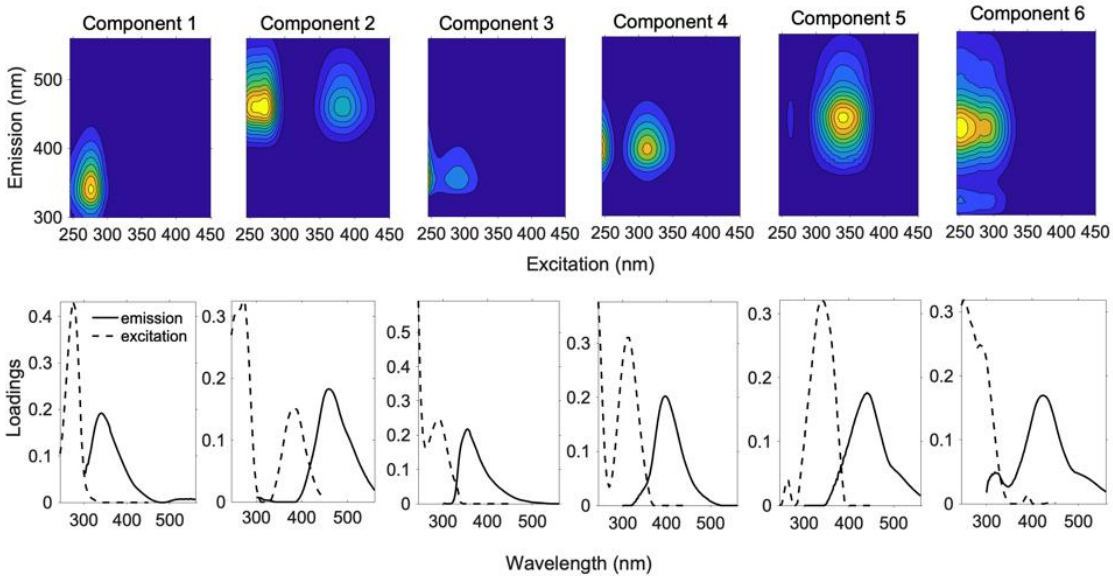

Fig S2 *PARAFAC model results showing fluorescence fingerprint of six components (upper panel) and excitation emission spectra (lower panel)*

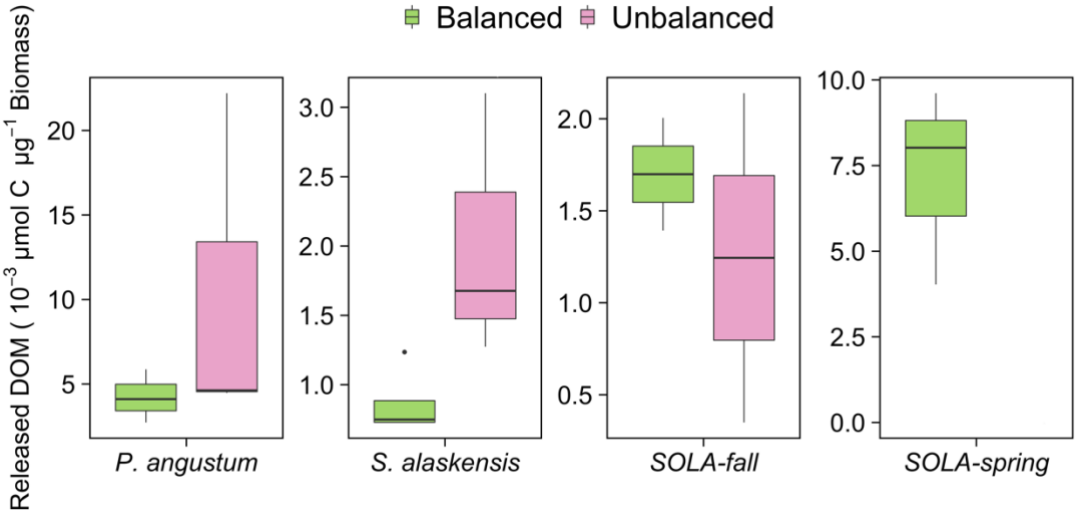

Fig S3 *Dissolved organic matter release at the end of the experiment expressed as DOC concentration per unit of integrated biomass (T_0 to T_f) in all experiments. Hinges correspond to median, first and third quartiles. Whiskers extended from hinges to the smallest and largest values (no further than 1.5 * IQR from the hinge, where IQR is the inter-quartile range.* ***No significant difference between balanced an unbalanced over all experiments (ANOVA, p-value >0.1).***

Supplementary references

Aminot, A., and R. Kérouel. 2007. *Dosage Automatique Des Nutriments Dans Les Eaux Marines. Méthodes En Flux Continu*. Ifremer-Quae.

Benner, Ronald, and Michael Strom. 1993. "A Critical Evaluation of the Analytical Blank Associated with DOC Measurements by High-Temperature Catalytic Oxidation." *Marine Chemistry*, Measurement of Dissolved Organic Carbon and Nitrogen in Natural Waters, 41 (1): 153–60. https://doi.org/10.1016/0304-4203(93)90113-3.

Bittar, Thais B., Stella A. Berger, Laura M. Birsa, Tina L. Walters, Megan E. Thompson, Robert G. M. Spencer, Elizabeth L. Mann, Aron Stubbins, Marc E. Frischer, and Jay A. Brandes. 2016. "Seasonal Dynamics of Dissolved, Particulate and Microbial Components of a Tidal Saltmarsh-Dominated Estuary under Contrasting Levels of Freshwater Discharge." *Estuarine, Coastal and Shelf Science* 182 (December): 72–85. https://doi.org/10.1016/j.ecss.2016.08.046.

Brym, Adeline, Hans W. Paerl, Michael T. Montgomery, Lauren T. Handsel, Kai Ziervogel, and Christopher L. Osburn. 2014. "Optical and Chemical Characterization of Base-Extracted Particulate Organic Matter in Coastal Marine Environments." *Marine Chemistry* 162 (May): 96–113. https://doi.org/10.1016/j.marchem.2014.03.006.

Catalá, Teresa S., Isabel Reche, Cintia L. Ramón, Àngel López-Sanz, Marta Álvarez, Eva Calvo, and Xosé A. Álvarez-Salgado. 2016. "Chromophoric Signatures of Microbial By-Products in the Dark Ocean: MICROBIAL CHROMOPHORIC SIGNATURES." *Geophysical Research Letters* 43 (14): 7639–48. https://doi.org/10.1002/2016GL069878.

Catalán, Núria, Ada Pastor, Carles M. Borrego, Joan Pere Casas-Ruiz, Jeffrey A. Hawkes, Carmen Gutiérrez, Daniel von Schiller, and Rafael Marcé. 2021. "The Relevance of Environment vs. Composition on Dissolved Organic Matter Degradation in Freshwaters." *Limnology and Oceanography* 66 (2): 306–20. https://doi.org/10.1002/lno.11606.

Coble, Paula G. 2007. "Marine Optical Biogeochemistry: The Chemistry of Ocean Color." *Chemical Reviews* 107 (2): 402–18. https://doi.org/10.1021/cr050350+.

Du, Yingxun, Yuanyuan Zhang, Feizhou Chen, Yuguang Chang, and Zhengwen Liu. 2016. "Photochemical Reactivities of Dissolved Organic Matter (DOM) in a Sub-Alpine Lake Revealed by EEM-PARAFAC: An Insight into the Fate of Allochthonous DOM in Alpine Lakes Affected by Climate Change." *Science of The Total Environment* 568 (October): 216–25. https://doi.org/10.1016/j.scitotenv.2016.06.036.

Eguchi, Mitsuru, Martin Ostrowski, Fitri Fegatella, John Bowman, David Nichols, Tomohiko Nishino, and Ricardo Cavicchioli. 2001. "Sphingomonas Alaskensis Strain AFO1, an Abundant Oligotrophic Ultramicrobacterium from the North Pacific." *Applied and Environmental Microbiology* 67 (11): 4945–54. https://doi.org/10.1128/AEM.67.11.4945-4954.2001.

Fagerbakke, Km, M Heldal, and S Norland. 1996. "Content of Carbon, Nitrogen, Oxygen, Sulfur and Phosphorus in Native Aquatic and Cultured Bacteria." *Aquatic Microbial Ecology* 10: 15–27. https://doi.org/10.3354/ame010015.

Fukuda, Rumi, Hiroshi Ogawa, Toshi Nagata, and Isao Koike. 1998. "Direct Determination of Carbon and Nitrogen Contents of Natural Bacterial Assemblages in Marine Environments." *Applied and Environmental Microbiology* 64 (9): 3352–58. https://doi.org/10.1128/AEM.64.9.3352-3358.1998.

Gonçalves-Araujo, Rafael, Colin A. Stedmon, Birgit Heim, Ivan Dubinenkov, Alexandra Kraberg, Denis Moiseev, and Astrid Bracher. 2015. "From Fresh to Marine Waters: Characterization and Fate of Dissolved Organic Matter in the Lena River Delta Region, Siberia." *Frontiers in Marine Science* 2: 108. https://doi.org/10.3389/fmars.2015.00108.

Lapierre, J.-F., and P. A. del Giorgio. 2014. "Partial Coupling and Differential Regulation of Biologically and Photochemically Labile Dissolved Organic Carbon across Boreal Aquatic Networks." *Biogeosciences* 11 (20): 5969–85. https://doi.org/10.5194/bg-11-5969-2014.

Lee, Sanghoon, and Jed A. Fuhrman. 1987. "Relationships between Biovolume and Biomass of Naturally Derived Marine Bacterioplankton." *Applied and Environmental Microbiology* 53 (6): 1298–1303.

Murphy, Kathleen R., Adam Hambly, Sachin Singh, Rita K. Henderson, Andy Baker, Richard Stuetz, and Stuart J. Khan. 2011. "Organic Matter Fluorescence in Municipal Water Recycling Schemes: Toward a Unified PARAFAC Model." *Environmental Science & Technology* 45 (7): 2909–16. https://doi.org/10.1021/es103015e.

Murphy, Kathleen R., Colin A. Stedmon, Daniel Graeber, and Rasmus Bro. 2013. "Fluorescence Spectroscopy and Multi-Way Techniques. PARAFAC." *Analytical Methods* 5 (23): 6557–66. https://doi.org/10.1039/C3AY41160E.

Murphy, Kathleen R., Colin A. Stedmon, Philip Wenig, and Rasmus Bro. 2014. "OpenFluor– an Online Spectral Library of Auto-Fluorescence by Organic Compounds in the Environment." *Analytical Methods* 6 (3): 658–61. https://doi.org/10.1039/C3AY41935E.

Myklestad, Sverre M., Elin Skånøy, and Solveig Hestmann. 1997. "A Sensitive and Rapid Method for Analysis of Dissolved Mono- and Polysaccharides in Seawater." *Marine Chemistry*, Modern Chemical and Biological Oceanography: The Influence of Peter J. Wangersky, 56 (3): 279–86. https://doi.org/10.1016/S0304-4203(96)00074-6.

Osburn, Christopher L., Diana Oviedo-Vargas, Emily Barnett, Diego Dierick, Steven F. Oberbauer, and David P. Genereux. 2018. "Regional Groundwater and Storms Are Hydrologic Controls on the Quality and Export of Dissolved Organic Matter in Two Tropical Rainforest Streams, Costa Rica." *Journal of Geophysical Research: Biogeosciences* 123 (3): 850–66. https://doi.org/10.1002/2017JG003960.

Stedmon, Colin A., and Stiig Markager. 2005. "Resolving the Variability in Dissolved Organic Matter Fluorescence in a Temperate Estuary and Its Catchment Using PARAFAC Analysis." *Limnology and Oceanography* 50 (2): 686–97. https://doi.org/10.4319/lo.2005.50.2.0686.

Wang, Hui, Zhongqiao Li, Wan-E Zhuang, Jin Hur, Liyang Yang, and Yonghao Wang. 2020. "Spectral and Isotopic Characteristics of Particulate Organic Matter in a Subtropical Estuary under the Influences of Human Disturbance." *Journal of Marine Systems* 203 (March): 103264. https://doi.org/10.1016/j.jmarsys.2019.103264.

Yamashita, Youhei, Rudolf Jaffé, Nagamitsu Maie, and Eiichiro Tanoue. 2008. "Assessing the Dynamics of Dissolved Organic Matter (DOM) in Coastal Environments by Excitation

Emission Matrix Fluorescence and Parallel Factor Analysis (EEM-PARAFAC).” *Limnology and Oceanography* 53 (5): 1900–1908. https://doi.org/10.4319/lo.2008.53.5.1900.